Japanese Journal of Applied Physics
Vol. 44, No. 2, 2005, pp. L 78–L 81

The Effect of N_2 Flow Rate in $He/O_2/N_2$ on the Characteristics of Large Area Pin-to-Plate Dielectric Barrier Discharge

Yong-Hyuk LEE*, Se-Jin KYUNG, Chang-Hyun JEONG and Geun-Young YEOM†

Department of Materials Sciences & Engineering, Sungkyunkwan University, Suwon, Korea

(Received October 4, 2004; accepted November 23, 2004; published December 17, 2004)

In this study, the effects of N_2 flow rate in the $He/O_2/N_2$ gas mixture on the characteristics of a pin-to-plate dielectric barrier discharge (DBD) having the size of 100 mm × 1000 mm have been investigated for the application to flat panel display processing such as photoresist ashing. The pin-to-plate DBD showed about 70–120% higher photoresist ashing rate at the same applied voltage compared to the conventional DBD. The addition of 3 slm of N_2 to He(10 slm)/O_2(3 slm) showed the highest photoresist ashing rate of about 580 nm/min for the pin-to-plate DBD at 12 kV of AC voltage. The increase of N_2 flow rate in He/O_2 gas mixture up to 3 slm appeared to increase the density of N_2^+ ions and N_2 metastables while the oxygen atomic density appeared to decrease continuously. The increase of photoresist ashing rate with the increase of N_2 flow rate up to 3 slm was related to the increase of the substrate surface temperature by the increased collision of N_2^+ ions and N_2 metastables with the substrate. [DOI: 10.1143/JJAP.44.L78]

KEYWORDS: corona discharge, DBD, atmospheric pressure plasma, $He/O_2/N_2$, OES

Currently, low pressure plasma processing is widely used for semiconductor and flat panel display industries in the areas of etching, deposition, cleaning, etc.[1–5] However, in the case of the flat panel display industries, due to the extremely large size of the substrate, problems such as the high cost of ownership of the plasma processing system, the difficulty in the fabrication of the extremely large area vacuum system, non-uniformity of the plasma, etc. are encountered for the plasma processing of next generation substrates. One of the possible solutions is to use atmospheric pressure plasmas that do not need costly vacuum equipments and can process in-line without using a loadlock. Also, due to the cost and environmental problems of wet chemicals, wet cleaning processes are also considered to be replaced by atmospheric pressure plasma cleaning.[6–9)]

Among the various atmospheric pressure plasmas, dielectric barrier discharge (DBD) which has dielectric plates on one or both of the parallel electrodes is generally applied to semiconductors and flat panel displays because it is a glow discharge-type that can have a uniform plasma over the substrate area. However, the conventional DBD has a high breakdown voltage (30 kV/cm at air) and a low plasma density due to the high recombination rate at the atmospheric pressure, therefore, it is difficult to apply various major plasma processing such as etching and deposition except for surface treatment.[10–14]

In this study, a modified DBD consisted of multi-pin power electrode instead of planar power electrode (pin-to-plate DBD) was used to generate high density plasmas at low breakdown voltage and the effects of N_2 addition to He/O_2 on the characteristics of plasma and photoresist ashing were investigated for the application to large area flat panel display processing.

Figure 1 shows the schematic diagram and electric diagram (*Q-V* Lissarjou) of the system used in the experiment. The discharge system was composed of multi-pin top powered electrode and blank ground electrode and both electrodes were covered with 3 mm thick quartz plate. The air gap between the electrodes was 4 mm. The size of electrode was 100 mm length × 1000 mm width for the application to the flat panel display. 12 kV of AC power (20–30 kHz) was applied to the powered multi-pin electrode to generate atmospheric pressure plasmas.

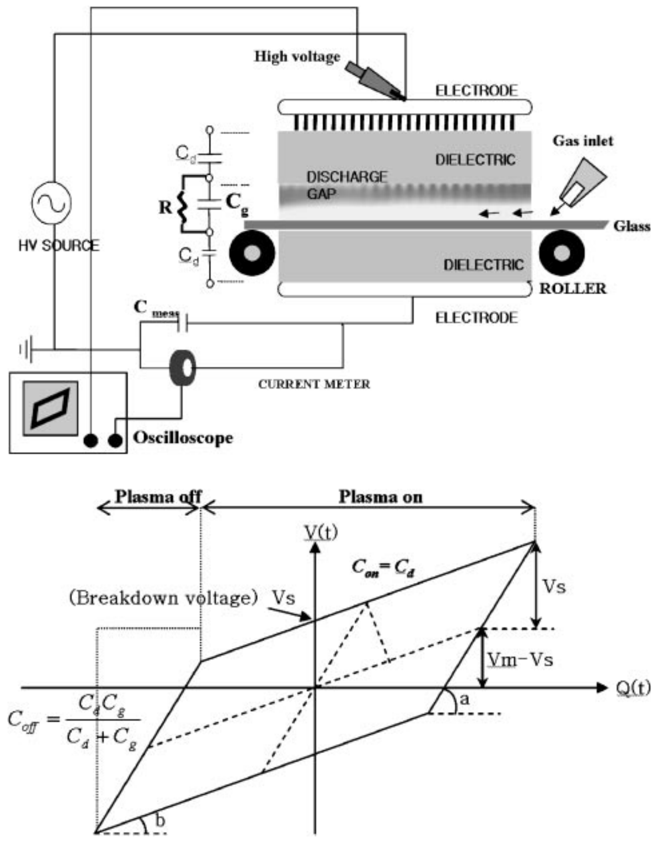

Fig. 1. (a) Schematic diagram of the atmospheric pressure plasma system (pin-to-plate type) and (b) the *Q-V* Lissarjou curve (*Q-V* oscillographic diagram) investigated in this study.

As the discharge gas, mixtures of 10 slm of He, 3 slm of O_2, and 0 to 5 slm of N_2 were used. The characteristics of the atmospheric pressure plasmas were measured using a high voltage probe (Tektronix P6015A), a current probe (Pearson

*E-mail address: yhlee73@skku.edu
†E-mail address: gyyeom@skku.ac.kr

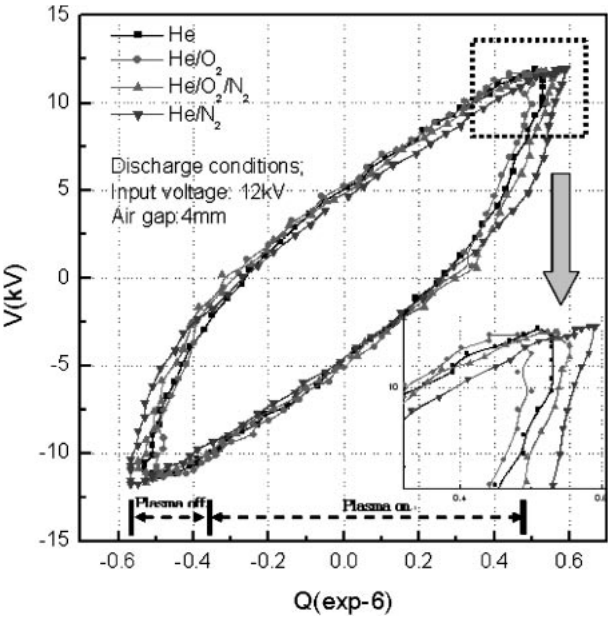

Fig. 2. *Q-V* Lissajou curves of the discharges for the gas mixtures of He(10 slm), He(10 slm)/O_2(3 slm), He(10 slm)/N_2(3 slm), and He(10 slm)/O_2(3 slm)/N_2(3 slm) for the pin-to-plate type DBD having the electrode size of 100 mm × 1000 mm.

electronics 6600), and by investigating *Q-V* (charge-voltage) Lissajou plot using a capacitor ($C_{meas} = 0.45\,\mu F$) attached to the circuit as shown in the figure. Species in the plasmas were investigated using optical emission spectroscopy (OES, SC Tech. PCM-420). To measure the photoresist ashing rates, 1.4 µm thick photoresist covered amorphous silicon/glass substrates were used and were positioned on the dielectric plate of the ground electrode using an in-line roller system.

Figure 2 shows the measured *Q-V* Lissajou curves of the discharges for the gas mixtures of He(10 slm), He(10 slm)/O_2(3 slm), He(10 slm)/N_2(3 slm), and He(10 slm)/O_2(3 slm)/N_2(3 slm) at 12 kV of AC voltage for the pin-to-plate DBD. The capacitance of the discharge system ($C_{off} = \frac{C_d C_g}{C_d + C_g}$; capacitance of dielectric and air gap) obtained during the plasma-off period for He(10 slm)/O_2(3 slm) from the plot was about 280 pF and that during the plasma-on period ($C_{on} = C_d$; capacitance of dielectric) was about 812 pF for He(10 slm), 764 pF for He(10 slm)/O_2(3 slm), 844 pF for He(10 slm)/O_2(3 slm)/N_2(3 slm), and 897 pF for He(10 slm)/N_2(3 slm). Plasma breakdown voltages at 4 mm were about 5 kV and were similar for different gas mixtures, and the breakdown voltage was significantly lower than that by conventional DBD (about 6.3 kV). The half period of plasma-on time for He(10 slm)/N_2(3 slm) was about 0.960 µs; while that for He(10 slm)/O_2(3 slm) was 0.873 µs; and that for He(10 slm) was 0.929 µs;, therefore, the plasma-on time during the AC period was increased by the addition of N_2 while the addition of O_2 to He decreased the plasma-on time.

The addition of O_2 to He decreases plasma density by electron attachment to oxygen (electron attachment probability; He 0, N_2 0, O_2 10^{-4}, O 10^{-3}) even though oxygen atom is required for ashing of photoresist by the dissociation of oxygen molecules by the following reactions;

$$e + O_2 \rightarrow O + O^- \qquad (1)^{6)}$$

$$e + O_2 \rightarrow e + O_2(A^3\Sigma_u^+,\ or\ B^1\Sigma_u^- \rightarrow e + 2O \qquad (2)^{6)}$$

$$e + O_2^+ \rightarrow O + O \qquad (3)^{14)}$$

Also, it was reported that, from the following reaction, oxygen atoms in the plasma decrease the N_2 metastables by acting as the quencher of N_2 metastables.

$$O(^3P) + N_2(A_3\Sigma_u^+) \rightarrow O(^2S) + N_2(X\Sigma_g^+) \qquad (4)^{15)}$$

The addition of N_2 in He, however, increases the N_2 metastables by the reaction with He metastables and, by the reactions between the N_2 metastables, plasma density is increased from the following reactions;

$$e + N_2 \rightarrow e + N_2(A^3\Sigma_u^+,\ or\ a'^1\Sigma_u^-) \qquad (5)^{16)}$$

$$N_2(a'^1\Sigma_u^-) + N_2(A^3\Sigma_u^+,\ or\ a'^1\Sigma_u^-) \rightarrow N_4^+ + e \qquad (6)^{17)}$$

$$He^* + N_2 \rightarrow N_2^+(B_2\Sigma_u^+) + He + e \qquad (7)^{18)}$$

The decrease of plasma-on time for the O_2 addition and the increase of plasma-on time for the N_2 addition observed in the Fig. 2, therefore, are believed to be related to the decrease of plasma density by the electron attachment for the O_2 addition and the increase of N_2 metastables and the increase of plasma density for the N_2 addition to He. However, too high percentage of N_2 in the He can cause the increase of plasma breakdown voltage due to the high breakdown voltage of N_2 gases (the breakdown voltage/mm relative to nitrogen N_2 1, He 0.15, O_2 0.92, air (flat electrode) 3.0, and Ar 0.18).

Figure 3 shows the effect of N_2 flow rate in the He(10 slm)/O_2(3 slm)/N_2(0∼5 slm) gas mixture on the relative optical emission intensities of He(706.5 nm), O(777 nm), N_2^+(391 nm), N_2(337 nm), and NO(230∼280 nm; NO_γ system [$A^2\Sigma+ \rightarrow X^2\Pi$]) measured by OES. As shown in the figure, the increase of N_2 gas flow rate in

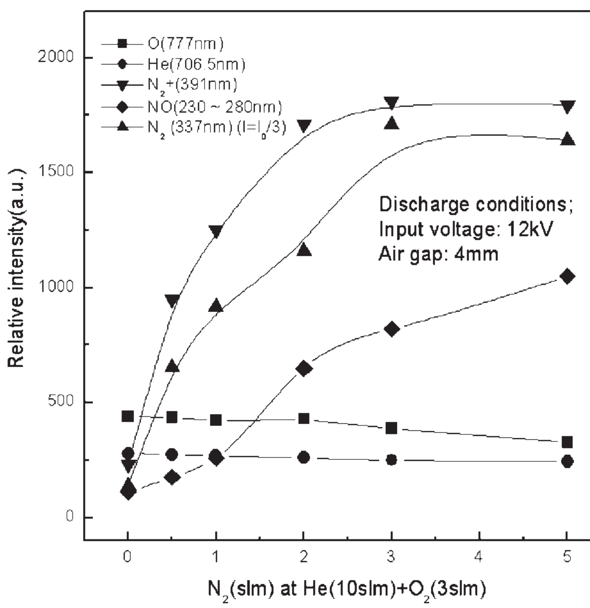

Fig. 3. Effect of N_2 flow rate in the He(10 slm)/O_2(3 slm)/N_2(0∼5 slm) gas mixture on the relative optical emission intensities of He(706,5 nm), O(777 nm), N_2^+(391 nm), N_2(337 nm), and NO(230∼280 nm; NO_γ system) measured by OES.

the gas mixtures increased the emission intensities of N_2 and N_2^+ until 3 slm of N_2 was added and the further increase of N_2 did not change the intensities significantly. In the case of He and O, the increase of N_2 in the gas mixture continuously decreased the intensities from He and O. The increase of emission peaks from N_2 and N_2^+ with the increase of N_2 flow rate up to 3 slm is related to the increase of N_2 percentage in the gas mixture. Also, the decrease of emission peaks from He and O is related to the decrease of He and O percentage in the gas mixture with the increase of N_2 flow rate. However, the saturation of the emission peaks of N_2 and N_2^+ appears related to the onset of filamentary discharge due to the high N_2 percentage in the gas mixture. Too high N_2 percentage in the gas mixture increases breakdown voltage and increases temperature of the gases, therefore, it appears to change from glow discharge to filamentary discharge when N_2 gas flow rate is high enough. In the OES, NO emission peak was also observed and the peak intensity was increased with the increase of N_2 flow rate. NO is formed by the following reactions;

$$N_2 + O \rightarrow NO + N \qquad (8)^{15)}$$

$$N + O_2 \rightarrow NO + O \qquad (9)^{13)}$$

Therefore, the decrease of oxygen atomic intensity with the increase of N_2 is also related to the consumption of oxygen atoms and molecules by the formation of NO.

Figure 4 shows the effects of N_2 flow rate in the He(10 slm)/O_2(3 slm)/N_2(0∼5 slm) gas mixture on the etch rates of photoresist and discharge root-mean-square (rms) currents at 12 kV of applied voltage. As a reference, the etch rates and discharge currents of a conventional DBD was included. The DBD was formed by replacing the multi-pin power electrode with a blank plate electrode. As shown in the figure, the etch rate of photoresist was increased significantly until 3 slm of N_2 was added to the He(10 slm)/O_2(3 slm), however, the further increase of N_2 flow rate decreased the photoresist etch rate slightly for both the conventional DBD and pin-to-plate DBD. However, the pin-to-plate DBD showed about 70–120% higher etch rate compared to the conventional DBD for all of the conditions. The highest photoresist etch rate obtained in this study was about 580 nm/min at He(10 slm)/O_2(3 slm)/N_2(3 slm) with 12 kV of applied voltage for the pin-to-plate DBD. The discharge current measured using a current probe also showed the similar trend as the etch rates. When the consumed power was calculated, the consumed power at a fixed voltage was about 40% higher for the pin-to-plate DBD. Therefore, if the energy cost during the photoresist etching is compared, the pin-to-plate DBD was more efficient compared to the conventional parallel plate DBD.

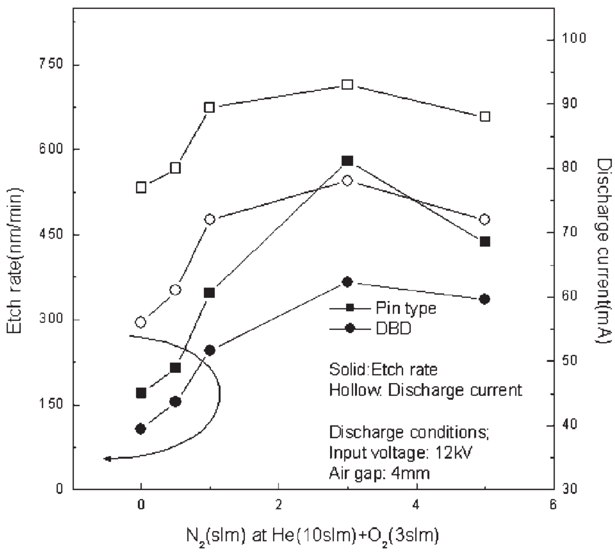

Fig. 4. Effects of N_2 flow rate in the He(10 slm)/O_2(3 slm)/N_2(0∼5 slm) gas mixture on the etch rates of photoresist and discharge rms currents at 12 kV of applied voltage. As a reference, the etch rates and discharge currents of a conventional DBD was included.

With increasing N_2 flow rate, the oxygen atomic density was decreased due to the decrease of oxygen percentage in the gas mixture and by the reaction of N with oxygen atoms as mentioned above. Therefore, the increase of N_2 flow rate did not increase oxygen atomic density which can react with photoresist. However, the increase of N_2^+ and N_2 metastables with increasing N_2 flow rate up to 3 slm N_2 shown in Figure 3 can increase the substrate surface temperature by the collision of the ions and metastables with the substrate. In fact, when the substrate temperature was measured after 3 min of operation, with the increase of N_2 from 0 to 3 slm, the increase of substrate surface temperature from 50°C to 70°C could be observed by a thermometer. Therefore, the increase of photoresist etch rate with increasing N_2 flow rate up to 3 slm is believed to be related to the increased collision of N_2^+ ions and N_2 metastables to the substrate due to the higher N_2^+ ion and N_2 metastable densities. The similar trend of current density with that of the etch rate also shows the increased ion density and the increased collision of ions to the substrate. The decrease of photoresist etch rate above 3 slm of N_2 is also related to the decrease of N_2^+ and N_2 metastables due to the change of discharge from a glow discharge to a filamentary discharge.

In summary, as the application to flat panel display processing such as photoresist ashing, the effects of N_2 flow rate in He/O_2/N_2 gas mixtures on the characteristics of a pin-to-plate DBD having the size of 100 mm × 1000 mm have been investigated. The addition of N_2 of 3 slm to He(10 slm)/O_2(3 slm) increased the plasma-on time possibly due to the increase of N_2^+ ions and N_2 mestastables as observed by the OES. However, the increase of N_2 decreased the oxygen atomic density due to the decrease of oxygen percentage in the gas mixture and due to the reaction of oxygen with N_2. The addition of 3 slm of N_2 to He(10 slm)/O_2(3 slm) showed the highest photoresist ashing rate of about 580 nm/min for the pin-to-plate DBD. The increase of photoresist ashing rate with the increase of N_2 flow rate up to 3 slm was related to the increase of the substrate surface temperature by the increased collision of N_2^+ ions and N_2 metastables with the substrate.

This work was supported by the National Research Laboratory Program by Korea Ministry of Science and Technology (MOST).

1) S. Kanazawa, M. Kogoma, T. Moriwaki and S. Okazaki: J. Phys. D **21** (1988) 838.
2) N. K. Bibinov, A. A Fateev and K. Wiesemann: J. Phys. D **34** (2001) 1819.
3) Y. H. Lee, C. H. Yi, M. J. Chung and G. Y. Yeom: Surf. Coat. Tech.

146 (2001) 474.
4) C. H. Yi, Y. H. Lee and G. Y. Yeom: Surf. Coat. Tech. **171** (2003) 237.
5) F. Massines, A. Rabehi, P. Decomps, R. B. Gadri, P. Segur and C. Mayoux: J. Appl. Phys. **83** (1998) 2950.
6) S. Wang, V. Schulz-von der Gathen and H. F. Dobele: Appl. Phys. Lett. **83** (2003) 3272.
7) S. K. Dhali and I. Saradja: J. Appl. Phys. **69** (1991) 6319.
8) F. Massines, P. Segur, N. Gherardi, C. Khamphan and A. Richard: Surf. Coat. Tech. **174** (2003) 8.
9) H. E. Wagner, R. Brandenburg, K. V. Kozlov, A. Sonnenfeld, P. Michel and J. F. Behnke: Vacuum **71** (2003) 417.
10) J. S. Chang, P. A. Lawless and T. Yamamoto: IEEE Transactions on Plasma Sci. **19** (2001) 1152.
11) J. R. Roth: *Industrial Plasma Engineering* (Institute of Physics Publishing, Bristol, 2001).
12) S. C. Brown: *Basic Data of Plasma Physics* (American Vacuum Society Classics, USA, 1994).
13) M. Schmidt and K. H. Schoenbach: *Low Temperature Plasma Physics* (WILEY-VCH, Germany, 2001).
14) A. B. Rakshit *et al*: J. Phys. B **11** (1978) 4237.
15) I. A. Kossyi, A. Y. Kostinsky, A. A. Matveyev and V. O. Silakov: Plasma Sources Sci. Technol. **1** (1992) 207.
16) Y. B. Golubovskii, V. A. Maiorov, J. Behnke and J. F. Behnke: J. Phys. D **36** (2003) 39.
17) B. F. Gordiets, C. M. Ferreira, V. L. Guerra, J. M. A. Loureiro, J. Nahorny, D. Pagnon, M. Touzeau and M. Vialle: IEEE Transactions on Plasma Science **23** (1995) 750.
18) N. Gherardi, G. Gouda, E. Gat, A. Ricard and F. Massines: Plasma Sources Sci. Technol. **9** (2000) 340.